Biointerface Research in Applied Chemistry
Open-Access Journal (ISSN: 2069-5837)

Article
Volume 13, Issue 1, 2023, 94
https://doi.org/10.33263/BRIAC131.094

ERp57 Protein Activators for Management of Fertility by Virtual Screening and Molecular Dynamic Studies

Sahar Marashi [1], Arash Amanlou [2], Faezeh Sadat Hosseini [1], Nida Akhavan [3], Ramin Rahimnia [3,*], Massoud Amanlou [1,2,*]

[1] Department of Medicinal Chemistry, Faculty of Pharmacy, Tehran University of Medical Sciences, Tehran, Iran
[2] Experimental Medicine Research Center, Tehran University of Medical Sciences, Tehran, Iran
[3] Department of Medical Nanotechnology, Faculty of Advanced Sciences and Technology, Medical Sciences Branch, Islamic Azad University (IAUMS), Tehran, Iran
[4] Department of Medical Nanotechnology, School of Advanced Technologies in Medicine, Tehran University of Medical Sciences, Tehran, Iran
* Correspondence: rrahimnia@tums.ac.ir (R.R.); amanlou@tums.ac.ir (M.A.);

Scopus Author ID 6603321293
Received: 9.12.2021; Accepted: 3.01.2022; Published: 12.02.2022

Abstract: Objective(s): Infertility is a highly complex disorder of the genitalia with important medical and psychological issues. –Despite many efforts to treat infertility, pregnancy outcomes are meager (<12%). Defective sperm-Zona Pellucida (ZP) binding and penetration are the leading causes of zero fertilization rates. ERp57, a protein disulfide isomerase, is on the surfaces of spermatozoa, which enables sperm to penetrate the ZP. Up-regulation of the surface thiol content regulates human spermatozoa-ZP binding. ERp57 is a part of a spermatozoa-ZP receptor complex and a protein disulfide isomerase that regulates the thiol-disulfide exchange reactions of proteins. The binding site of calcitriol on the surfaces of ERp57 plays an indirect role in male fertility. Docking was used to finding calcitriol's possible binding mode on ERp57 and generate the structure-based pharmacophore model. Then the developed model was used to screen the Maybridge library to find non-steroidal analogs of calcitriol. Subsequently, forty-eight compounds were matched to the pharmacophore model and retrieved from the Maybridge library. All retrieved compounds were docked on the ERp57 binding pocket to analyze the molecular interactions and binding energy. The top twenty compounds with the highest binding energy were chosen for further analysis. Three compounds were selected for further evaluation by molecular dynamic simulation for 50 nanoseconds. Finally, compound 20, (2-[1-[4-(2-Methylpropyl)phenyl]ethyl]-5-(3-nitrophenyl)-1,3,4-oxadiazole) with higher similarity to calcitriol provides proper complex stability during the time of simulations, binding affinity, and binding energy even better than the calcitriol, in the active site of ERp57. Compound 20 with 1,3,4-oxadiazole core was introduced as a novel and potential ERp57 agonist to treat ERp57-related infertility.

Keywords: ERp57 activator; fertility; docking; calcitriol; virtual screening; molecular dynamic simulation.

1. Introduction

In humans, infertility is a disease of the male or female reproductive system defined by the failure to conceive a pregnancy after one year or more of regular and unprotected sexual intercourse [1,2]. Accordingly, one in every four (25%) couples in emerging countries were affected by infertility. The causes of infertility tend to differ in every country and population due to their lifestyle factors, such as age, smoking, weight, alcohol consumption. These factors

may result in a wide range of diagnosis problems, including ovulatory disorders, utero-tubal-peritoneal factors, and changes in sperm characteristics such as morphology, total count, motility, and unexplained infertility [3].

Many studies have been attempting to recognize the reasons for infertility and to apply assisted reproductive technologies (ARTs) such as in-vitro fertility (IVF) or intracytoplasmic sperm injection (ICSI) to treat this condition. Although IVF has been considered the most effective infertility treatment, the outcome of pregnancy in every IVF cycle has a low success rate of 34.3%[4]. In 70% of couples with the complete IVF failure, spermatozoa bound per Zona-Pellucida (ZP) is less than 5, and in 43%, the amount of sperm-Zona-Pellucida penetration reaches zero [5,6]. It shows that defective sperm-ZP binding and penetration are the leading causes of zero fertilization rates in vitro. These studies also suggest that sperm-ZP binding and penetration failure are mainly due to spermatozoa abnormalities and not the oocyte. The mammalian ZP consists of three to four glycoproteins usually indicated ZP1, ZP2, ZP3, and ZP4. Zona pellucida (ZP) plays an essential role in the life span of the mature human oocyte that provides regular protection against polyspermia by regulating sperm function [7-15]. During sperm immigration from testes to the tubes, the immature and immotile spermatozoa change physiologically and biochemically [16-19]. By adding several proteins secreted from the male reproductive tract glands, the mature sperm can bind to the ZP, undergo an acrosome reaction, and eventually penetrate the ZP [20-22]. This phenomenon occurs mainly due to specific proteins on surfaces of both spermatozoa and oocytes, namely, IZUMO, integrin, ERp57, GPI, and tetraspanins (CD9, CD81, etc.) [23-26]. ERp57 has attracted interest among fertility researchers among these proteins over the past decades. It is found in the acrosome and flagella of non-acrosome reacted sperm and migrates to the equatorial segment after acrosome reaction; inhibitors such as anti-ERp57 antibodies reduce the rate of gamete fusion. The IVF studies indicate that fertile donors and IVF patients with a high fertilization rate do not differ in ERp57 expression, while patients with a low success rate have a significantly lower expression level [7,26-29]. The ERp57, also known as PDai3, GRP58, or D-MAARS, is a protein disulfide-isomerase (PDI) family with a multifunctional activity involved in disulfide isomerization and thiol oxidation in substrate proteins [30,31]. It is initially located in the endoplasmic reticulum (ER), where it participates in forming and reshuffling disulfide bonds in newly synthesized proteins [32-36]. The mechanism of ERp57 in gamete fusion is not yet completely understood; however, since the thiol-disulfide exchange is required in some viral membrane fusion system activation, a similar mechanism may occur in sperm-egg fusion[26,37-39]. Moreover, some proteins such as IZUMO and CD9 possess disulfide bonds in their extracellular domain and are possibly substrates of ERp57 [23,40-42]. In recent years, ERp57 has been identified as a cell surface receptor in an intestinal epithelial cell, responsible for the rapid response to 1,25-dihydroxy vitamin D3 or calcitriol by binding to this hormone [34,43,44].

Although ERp57 can interact with various molecules, the specific active site and target substrates have not yet been identified. The ERp57 includes four thioredoxin-like domains, abb′a′, where the domains a and a′ contain catalytic CGHC motifs and are capable of catalyzing oxidoreduction and thiol-disulfide exchange reaction. In contrast, b and b′ domains are non-catalytic domains [45].

There is an increasing body of evidence that expression of VD3 receptors and their metabolic enzymes as well as CYP2R1, CYP27B1, and CYP24A1, in the seminal duct, in male genitalia, especially in the interstitial cell, seminal vesicles, prostate, spinal cord, and in regions

of the sperm head suggest the critical roles of VD3 in men fertility and reproduction, also increase mRNA expression of vitamin D3 receptor (VDR) in the endometrium and ovarian tissues that stimulates the production of progesterone, estradiol, and estrogen and regulates human chorionic gonadotropin (HCG) expression and secretion in women, therefore the presence of an active form of vitamin D3, calcitriol is essential [46-48]. Accordingly, vitamin D3 plays an indirect role in male and female fertility by regulating calcium levels. In hypocalcemia, hypogonadotropic hypogonadism had seen, caused down-regulation of the testicle, reduced intracellular calcium levels, lower spermatozoa, and pathological histology of the gonads. Furthermore, when a controlled diet standardized serum calcium, the formation and maturation of spermatozoa in the testis had improved significantly [49-51].

Although calcitriol has been used to treat osteoporosis, hyperparathyroidism, and autoimmune diseases, the treatment is limited due to hypercalcemia and increased bone resorption Calcitriol is applied to treat osteoporosis, hyperthyroidism, and autoimmune diseases and possibly prevention from different types of cancer, but effective treatment is still limited due to hypercalcemia, increased bone resorption and may cause tissue calcification [52-54]. Several non-steroidal analogs of calcitriol have been synthesized to reduce the calcemic side effects, and their biological activities were reported. Several synthetic vitamin D analogs have been introduced to reduce the calcemic side effect versus an effective cytoprotective and immune system modulator [55-57]. Calcitriol consists of four major parts: The A-ring, the Seco B-ring, the C/D ring, and the side chain. (Figure 1) [58]. The non-C/D ring series is the first series of non-steroidal analogs of calcitriol. These analogs are characterized by removing the normal C- and D- rings and replacing them with a five-membered ring [59].

This study is based on a computer-aided drug design to identifying identify pharmacophore groups of calcitriol of the active site of the ERp57. By pharmacophore-based virtual screening, several compounds were extracted from the library. Then, each component was docked on the possible binding mode on the surface of protein ERp57 and was analyzed to retrieve the potential ERp57 agonist with high potential activity. Lastly, further molecular dynamic simulations (MDs) were performed to validate the docking result in an in-vitro environment. From the information of this study, we investigate a possible strategy to design a new agonist for ERp57 to enhance sperm-gamete fusion or the treatment of ERp57-related infertility.

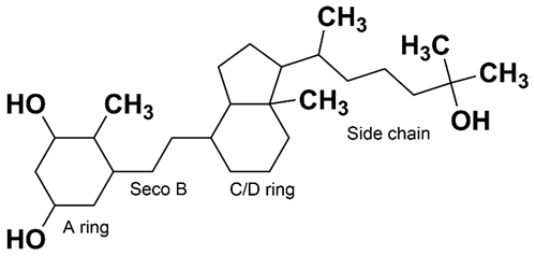

Figure 1. The structural section of calcitriol is shown above: A-ring, Seco-B, C/D ring, and side chain. The structure was generated by ChemDraw Ultra version 8.0, Chemical Communications Software, PerkinElmer.

2. Materials and Methods

2.1. Docking simulation procedure.

The original task of computational docking is to predict the possible binding mode of the interaction between ligand and receptor. The crystal structure of ERp57 was obtained from

the RCSB Protein Data Bank with PDB ID: 3F8U [60]. AutoDockTools (ADT) 1.5.6 package prepared the receptor and ligands input files [61]. The entire water molecule and ions were omitted from the crystal structure to prepare the receptor file. After adding the polar hydrogen, the Kollman charge was used for the partial atomic charge, and the PDBQT format was saved [62]. The 2D scaffolds of the ligand were drawn using Marvin Sketch v5.7 (ChemAxon). Afterward, all hydrogens were added, and the 3D structures of the molecules were molded. Non-polar hydrogens were merged, and Gasteiger charges parameters were assigned by default and saved in PDBQT format. The calculation of the binding free energies and conformation of the ligand on the defined active site was performed utilizing AutoDock Vina 1.1.2 [63]. In the first step, blind docking with the space dimension covering the entire protein was used to find the possible binding mode of calcitriol on ERp57. Then the most populated pose was selected for placement in the grid box for further investigation. The grid box dimensions were 46 × 30 × 30 Å (x, y, and z) with grid center -5.679, 75.195, and 62.815 (x, y, and z). The default values were set for the rest of the parameters.

2.2. Pharmacophore modeling.

The docking result used the complex of ERp57 and calcitriol with the lowest binding energy to generate the pharmacophore model. LigandScout version 3.0 was performed for structure-based model and virtual screening [64]. LigandScout allows making 3D pharmacophore models from structural data of ligand. It incorporates a complete definition of chemical features, such as hydrogen bond donors (HBD), acceptors (HBA), hydrophobic areas (HY), positively and negatively ionizable chemical groups, and aromatic ring (AR), which describes the interactions between a ligand and the binding site. A standard pharmacophore model was built to represent a structural requirement for the activity of the ERp57 activator (Figure 3). The pharmacophore model filtered the Maybridge library with approximately 55000 compounds. Forty-eight compounds were extracted and further investigated by docking and molecular dynamic simulation.

2.3. Molecular dynamics simulation.

GROMACS package 5.0.1 was applied to determine the ligand-protein interaction of three final selected compounds in a dynamic environment; ligands topology files were generated by the PRODRG web server [65]. The complex was placed in a dodecahedron shape box with the solvation of simple point charges (SPC) water molecules. Neutralization was done by adding Na+ or Cl- counter ions instead of water molecules. Energy minimization was submitted to the system with the steepest descent algorithm and 1000 kJ/mol/nm tolerance. NVT and NPT equilibration steps were also done. Finally, molecular dynamic simulation was run for 50 nanoseconds (ns), the GROMACS parameters and values were set similar to the previously published article [66].

3. Results and Discussion

3.1. Direct targeting.

To identify the potential binding site of calcitriol on the surface of protein ERp57, a blind docking was performed on the entire protein using AutoDock Vina 1.1.2. Blind docking is a practical approach to finding the binding site of biological targets [67,68]. Blind docking

predicted the binding pocket of calcitriol somewhere between the a and b domains of ERp57 with populated cluster and binding energy -8.1 kcal/mol (Figure 2). The binding pocket was surrounded with residues ASP250, ARG183, PHE148, VAL137, and LYS130 and was previously identified as one of the possible binding pockets of calcitriol on ERp57 by Gaucci *et al*. [33] and also the potential binding site of the diosgenin (a similar structure to the calcitriol) by Tohda *et al*. [69]. Table 1 shows the predicted binding pocket of the calcitriol by Gaucci *et al*.

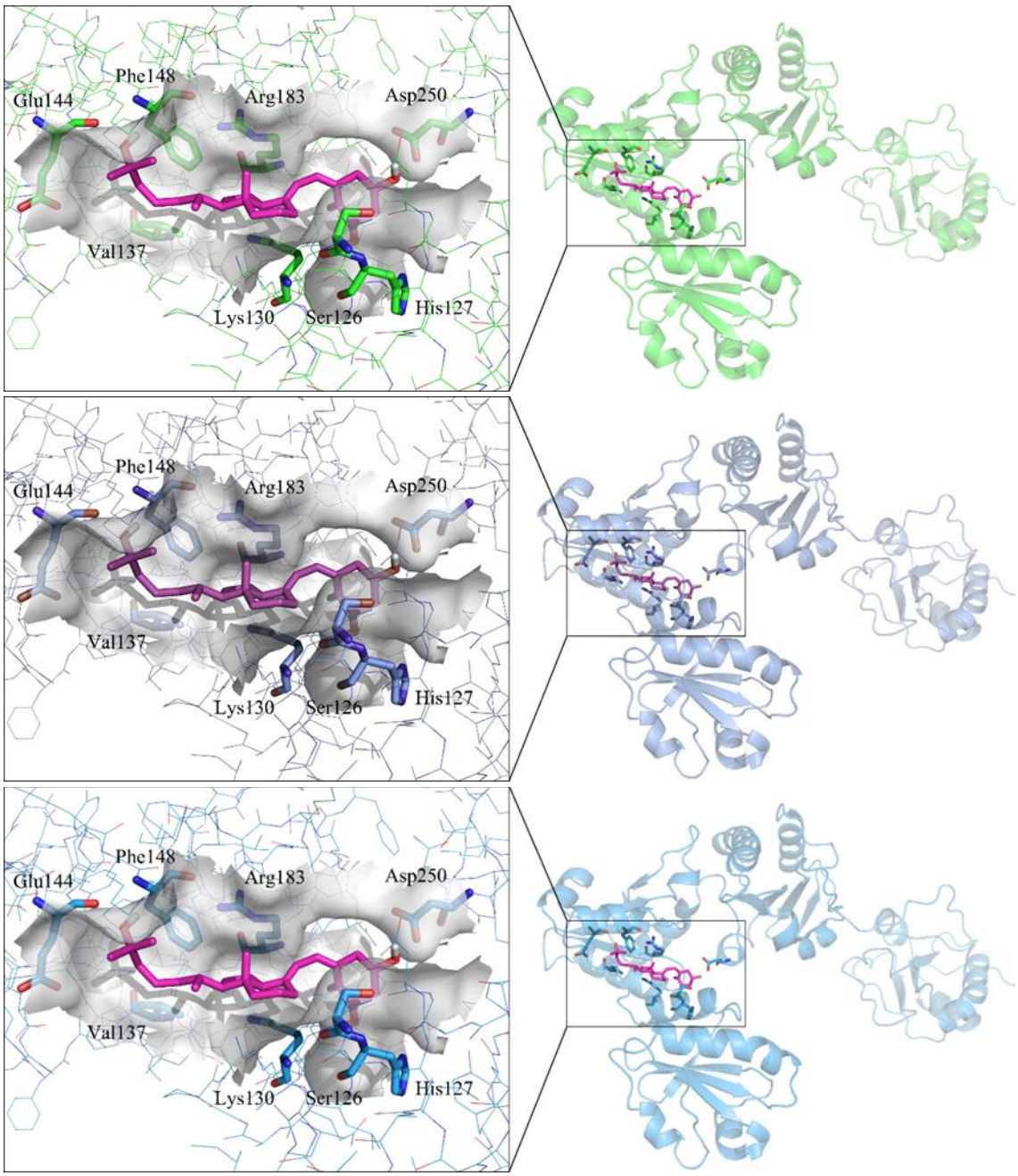

Figure 2. Binding mode of the most populated cluster of calcitriol on the groove area between a and b domain of ERp57. A picture was generated by the PyMol Molecular Graphics System version 1.1evel, Schrödinger, LLC. Available from: https://pymol.org.

Table 1. Predicted cavity and associated residue on ERp57.

Cavity No.	Available residues
Cavity 1	Arg207, Glu236, Asn239, Ile243, Cys244, Leu260, Glu273, Asn298, Ala300
Cavity 2	Lys130, Asp153, Arg179, Asp180, Asn181, Tyr182, Arg183
Cavity 3	Asp153,Ala154, Ser155, Asp180, Asn181, Tyr182, Ile240, Phe241, Leu254

Docking studies yielded important information about the orientation and interaction of the calcitriol. The docking result demonstrates that interaction between calcitriol and the receptor ERp57 involves several hydrophobic contacts and one hydrogen bond. The hydroxyl group of A-ring formed a hydrogen bond with Asp250, and the A-ring had hydrophobic interactions with Ser126 and His127 and Lys130, the methyl group next to the C/D ring made a hydrophobic interaction with Arg183 and the hydrophobic groups in side-chain positioned in a hydrophobic pocket formed by the residues Phe148 and Glu144 and Val137. Therefore, based on the binding pose, the structure-based pharmacophore model was generated, which contains structural features such as hydrogen bond donors (HBD), hydrophobic areas (HY), an aromatic ring (AR). The 2D and 3D representations of the pharmacophore model are shown in Figure 3.

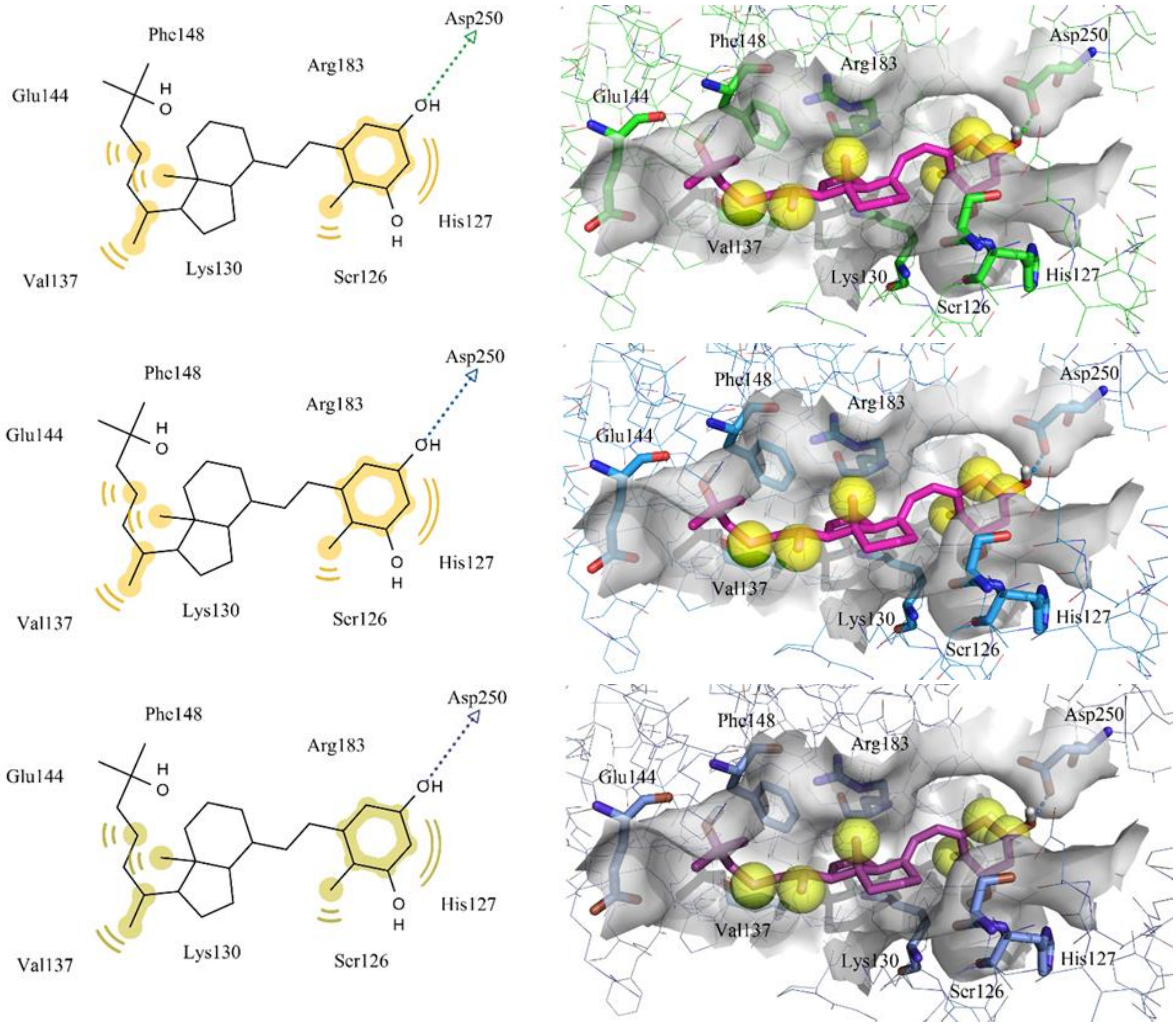

Figure 3. Pharmacophore model of the most populated binding mode of calcitriol on ERp57 in 2D and 3D representations. 2D pharmacophore model generated by LigandScout version 3.0 Inte; Ligand GmbH, and 3D representation generated by PyMol version 1.1evel.

3.2. Database screening and molecular docking.

The structure-based pharmacophore model created by LigandScout was used for virtual screening over the library of Maybridge containing 55000 compounds, and subsequently, forty-eight compounds were extracted based on the adaption score to the pharmacophore model. All extracted compounds were docked on the defined ERp57 surface binding pocket to analyze molecular interactions and binding energy. Docking results were sorted based on the binding energy value. Finally, twenty-first compounds with the lowest binding energy were selected

for further investigation. The structures of these compounds in Figure 4 and their docking binding energies are represented in Table 2.

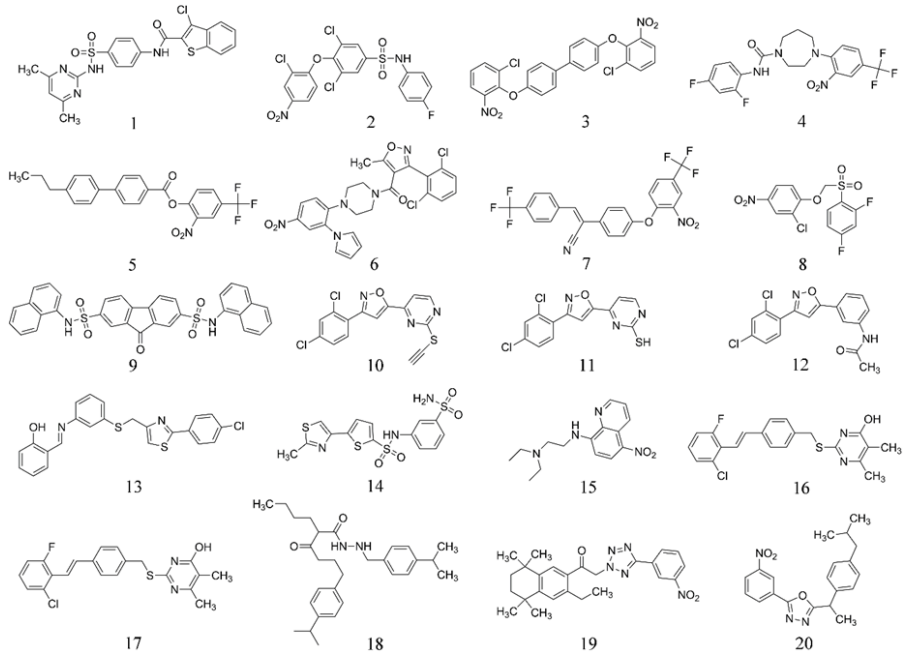

Figure 4. Structures of top twenty compounds from docking result. The structures were generated by ChemDraw Ultra version 8.0, Chemical Communications Software, PerkinElmer.

The following locations and orientation of the remaining compounds and their interactions into the binding site were analyzed. Eventually, compounds 12 (N-[3-[3-(2,4-Dichlorophenyl)-1,2-oxazol-5-yl]phenyl]acetamide), 13 (2-[[2-[[2-(4-Chlorophenyl)-1,3-thiazol-4-yl]methylsulfanyl]phenyl]iminomethyl]phenol), and 20 (2-[1-[4-(2-Methylpropyl)phenyl]ethyl]-5-(3-nitrophenyl)-1,3,4-oxadiazole) were selected for further investigation due to their ease of synthesis, favorable interactions with the binding site, and high binding affinity. The 3D interactions of the candidate compounds with ERp57 are shown in Figure 5.

Table 2. The calculated binding energy of 20 extracted compounds.

Compound	Binding Energy (kcal/mol)	Residues of Action	Compound	Binding Energy (kcal/mol)	Residues of Action
Calcitriol	-8.1	Asp250, His127, Ser126, Arg183, Val137	11	-7.2	Phe148, Leu139, Val137, Arg183, Asp151
1	-9.6	Ser126, Tyr115, His127, Val137, Phe148	12	-8.2	His127, Val137, Phe148, Asp250
2	-7.9	Val137, Lys147, Phe148, Ser126	13	-8.1	Val137, Phe148, Arg183, Asp250
3	-8.3	Phe148, Val137, Lys147, Arg179, Tyr182	14	-7.5	Phe148, Val137, Arg183, Arg179
4	-7.9	Phe148, Leu139, Val137, Asp153	15	-7.2	Val137, Ser126, Phe148, Tyr182
5	-8.4	Phe148, Arg183, Val137, Tyr182, Arg179, His127	16	-8.2	Phe148, Arg179, Val137
6	-8.0	Asp250, Asp151, Phe148, Val137	17	-8.4	Phe148, Leu139, Val137, Arg179
7	-8.8	Phe148, Leu139, Val137, Ser126	18	-9.8	Phe148, Leu139, Val137, Arg183, Tyr182
8	-7.3	His127, Arg183, Ser126, Phe148, Val137	19	-8.4	Asp53, Val137, Phe148, Tyr182, Ala154
9	-11.3	Leu139, Phe148, Val137, Ser126	20	-8.4	His127, Val137, Phe148, Arg183, Asp250
10	-7.6	Val137, Phe148, Arg179			

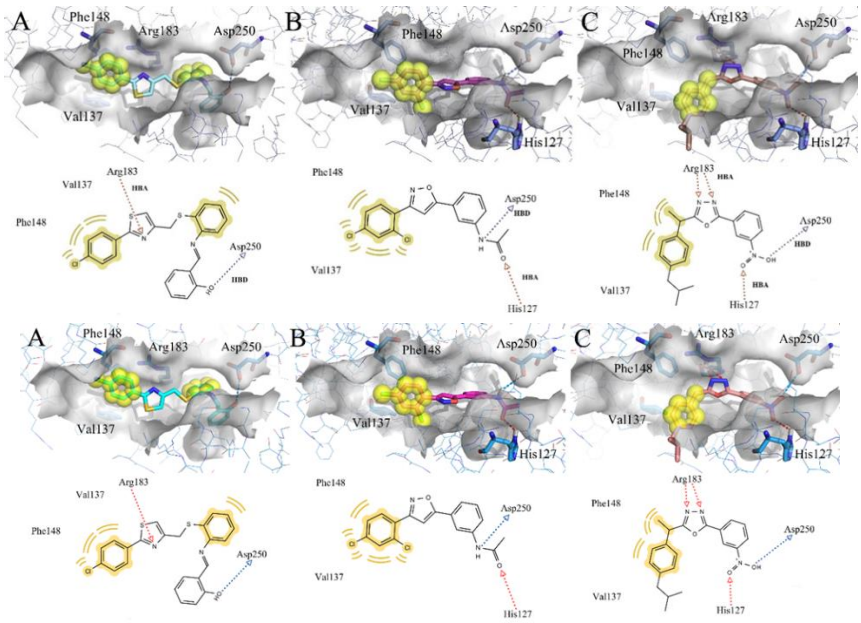

Figure 5. Binding orientation of compounds 13 (A), 12 (B), and 20 (C) and interactions they made with the active site of ERp57 protein. The blue and red lines are HBD and HBA features, respectively. Also, yellow spheres indicate the hydrophobic region. Two-dimensional representations; blue arrow: H-bond donor, red arrow: H-bond acceptor, yellow representation: hydrophobic site. 2D pharmacophore model generated by LigandScout version 3.0 Inte:Ligand GmbH, and 3D representation generated by PyMol version 1.1evel.

Analysis of the ligand-protein binding interaction indicates interactions with the binding site on ERp57 and the control compound calcitriol. The compound 13, positioned in a hydrophobic pocket formed by Arg183, Phe148, Val137, LYS130, and the hydroxyl group of phenol, made a hydrogen bond with Asp250 with the same binding energy -8.1 kcal/mol as calcitriol. Val37 and Phe148 sandwiched the chlorophenyl ring of compound 12, and the -NH group formed a hydrogen bond with Asp250. The binding energy of compound 12 was higher than calcitriol. In compound 20, the methyl and phenyl groups made hydrophobic interaction with hydrophobic cage surrounded by Arg183, Phe148, and Val137. Besides, four hydrogen bonds are formed with His127, Arg183, and Asp250 (Fig. 5), and the binding energy was -8.4 kcal/mol, which is higher than calcitriol -8.1 kcal/mol. In all three compounds, the C/D ring was replaced by a five-membered ring, causing these compounds to become non-steroidal analogs of calcitriol. Superimposed of each three compounds over calcitriol are shown in Figure 6.

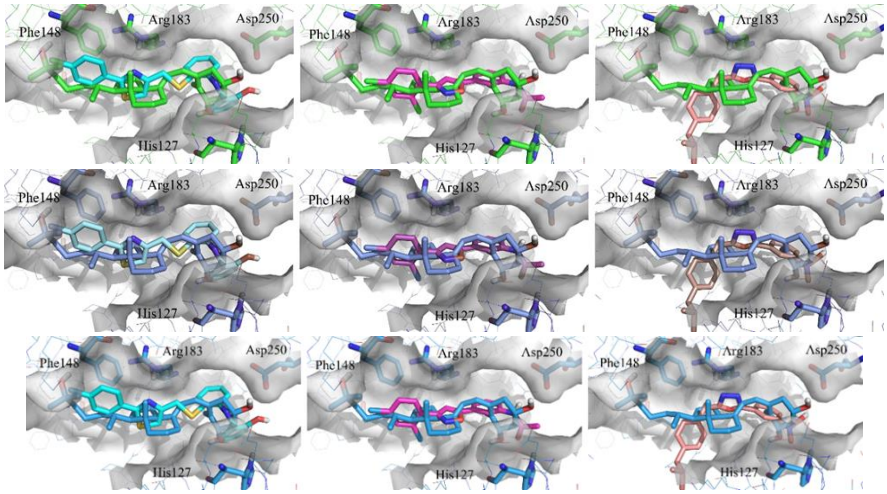

Figure 6. Superimposed compound 13 (cyan), 12 (magenta), and 20 (pink) over calcitriol (blue) on the binding site of ERp57. 3D representation generated by PyMOL version 1.1evel as well.

The docking results indicate that all three compounds could successfully fit into the target site of the protein ERp57. In general, there are no significant differences in terms of binding energy among selected compounds—compound 20 exhibits slightly lower binding energy than compounds 12 and 13 due to its hydrogen bonds. In addition, the structure of compound 20 is similar to the calcitriol with methyl group next to the 5-membered ring and also terminal dimethyl. Besides, a 5-carbon chain has been placed between the methyl group and dimethyl group in both structures. Therefore, compound 20 can probably mimic calcitriol properties better than others.

3.3. Molecular dynamics simulations.

To validate the docking result and the stability of ligands in the binding pocket of ERp57, 50 ns MD simulations were carried out on three selected compounds 12, 13, and 20 and the calcitriol. Accordingly, these compounds could be compared and calcitriol as an approved modulator of the ERp57. As observed in the backbone RMSD plot of protein in complex with ligands (Figure 7A), the protein with calcitriol reaches to equilibrate state for the last 20 ns of MD simulations as well as a protein with compound 20, which reached the steady-state around 30 ns of simulation. Still, the RMSD value increases as the time increases for two other compounds. Additionally, the ligand's RMSD plot of calcitriol (Figure 7B) indicated the stability of calcitriol during the study revealed the validity of predicted docking pose besides showing the accuracy of MD simulation is acceptable behavior from approved modulator of the ERp57. Compound 20 revealed a similar behavior pattern to calcitriol and was significantly stabilized. In contrast, two other compounds indicate significant fluctuations of RMSD value. Considering all the mentioned reasons, compound 20 could be a potent candidate for mimicking the calcitriol effect over the ERp57.

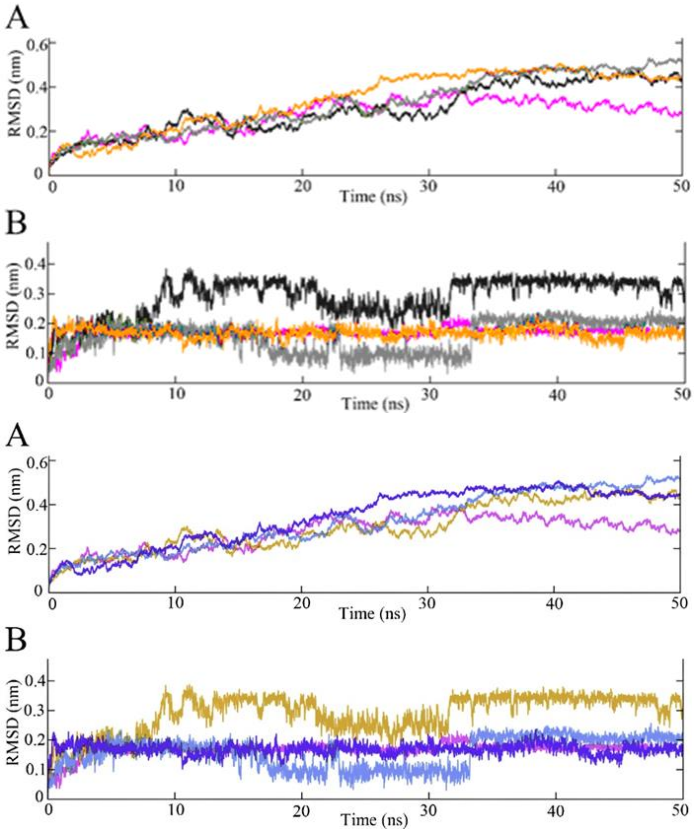

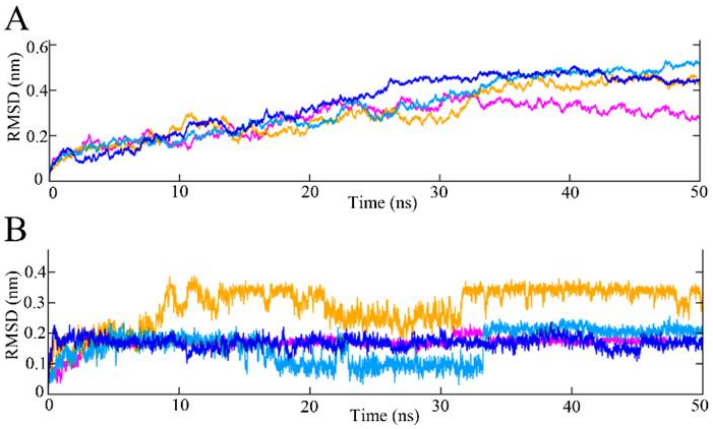

Figure 7. Molecular dynamic simulations plots for compound 20 (magenta), compound 12 (black), compound 13 (gray), and calcitriol (orange). (A) shows the movement of the protein backbone atoms and (B) the ligands atoms during the molecular dynamics simulations.

3.4. Discussion.

Infertility is a multifactorial disorder, and despite many attempts to treat it, the success rate of treatment is still very low. Most of the zero-rate fertilization is dependent on the defectiveness of sperm-Zona Pellucida (ZP) binding and penetration. The multifunctional ERp57, which is critical in this phenomenon, interacts with calcitriol and subsequently indirectly affects male fertility by regulating calcium levels. In addition, there is evidence that amyloid pathology is related to the cutting of the vitamin D/ERp57 pathway [70]. Other studies present the role of this pathway in Alzheimer's disease. Therefore, considering the notable role of interaction between ERp57 and vitamin D analogs in multiple malignancies, predicting the possible pose of the interaction can be very helpful.

In the present study, the possible binding pocket of calcitriol on the surface of ERp57 has been investigated, and our result was in good agreement with Tohda *et al*. and Gaucci *et al*. and predicted the hydrophobic binding pocket between a and b domains of ERp57.

Furthermore, calcitriol plays an essential role in regulating calcium homeostasis and has another role, such as antiproliferative effect on the normal and malignant cell. Besides, calcitriol improves the IVF cycle implantation process in infertile women with vitamin D deficiency [71].

Several structural analogs of calcitriol have been synthesized during the past decades, and some of them, such as tacalcitol and paricalcitol, is clinically approved to treat psoriasis and secondary hyperparathyroidism [71]. Interestingly, elocalcitol, a vitamin D3 analog, has been reported as a potential treatment for male infertility [72].

Because the interaction between calcitriol and ERp57 is effective on fertility, we tried to find new analogs of calcitriol for this purpose besides its already reported analogs. The structure-based pharmacophore model of calcitriol was generated with three main features, hydrogen bond donors (HBD), hydrophobic areas (HY), and an aromatic ring (AR). The model was used to screen the Maybridge library, and finally, forty-eight compounds were extracted and were docked to investigate possible interaction and binding energy. The top twenty compounds were evaluated for detailed interaction. Based on the docking result, all compounds indicated the hydrophobic interaction with Phe148 and Val137 due to aromatic rings in all compounds.

Nevertheless, substitute hydrogen bond donors like OH and NH groups form a strong hydrogen bond with critical Asp250. In addition, the interaction between His127 and Arg183

with the hydrogen bond acceptor group indicates an influential role in lowering the binding energy. Therefore compounds 12, 13, and 20 were selected based on the above-mentioned critical interaction and their ease of synthesis. Compounds 12, 13, and 20 contain the five-membered ring isoxazole, thiazole, and oxadiazole, respectively, which play the hydrogen bond, acceptor group. In the meantime, oxadiazole shows the ability to interact with both His127 and Arg183, which has caused differences in binding energy value compared to two other compounds. The following molecular dynamic simulation was performed to investigate the stability of the selected compounds in the binding pocket of ERp57. According to the RMSD plot, except for the complex of calcitriol, the complex with compound 20 reached a steady-state ahead of the two others. In the same manner, the ligand's RMSD plots confirmed that both calcitriol and compound 20 could fit the binding pocket and stabilize. Considering all the results mentioned above, compound 20 could be introduced as a potential analog of calcitriol to treat ERp57-related infertility.

4. Conclusions

In the current study, docking and pharmacophore modeling lead to investigate the possible site of the interactions of calcitriol on the active site of ERp57. Pharmacophore-based virtual screening retrieved the forty-eight compounds from the Maybridge library. All compounds were docked over the active site of the ERp57. The docking result was sorted based on the binding energy, and the top twenty compounds were evaluated for the binding modes and molecular interactions. After that, compounds with good binding affinity, favorable interaction with ERp57, and ease of synthesis were chosen as candidates for dynamic molecular studies. Finally, compound 20 (2-[1-[4-(2-Methylpropyl)phenyl]ethyl]-5-(3-nitrophenyl)-1,3,4-oxadiazole) with synthetic possibility, structural similarity with calcitriol, proper binding mode, and binding energy even better than the calcitriol, and stability in the active site during the simulation time, introduced as a novel and most likely analog of calcitriol. The findings of this study may be worth further studies to design new ERp57 agonists for the treatment of ERp57-related infertility. However, further study is still needed at the cellular level.

Funding

This research was funded by the Tehran University of Medical Sciences and Health Services.

Acknowledgments

This research has no acknowledgment.

Conflicts of Interest

The authors declare no conflict of interest.

References

1. Vander Borght, M.; Wyns, C. Fertility and infertility: Definition and epidemiology. *Clin. Biochem.* **2018,** *62*, 2-10, https://doi.org/10.1016/j.clinbiochem.2018.03.012.
2. Organization, W.H. LWW, **2021**.
3. Brugo-Olmedo, S.; Chillik, C.; Kopelman, S. Definition and causes of infertility. *Reprod Biomed Online* **2001,** *2*, 41-53, https://doi.org/10.1016/s1472-6483(10)62187-6.

4. Sullivan, R.; Legare, C.; Villeneuve, M.; Foliguet, B.; Bissonnette, F. Levels of P34H, a sperm protein of epididymal origin, as a predictor of conventional in vitro fertilization outcome. *Fertil Steril* **2006,** *85*, 1557-9, https://doi.org/10.1016/j.fertnstert.2005.10.070.
5. Liu, D.Y.; Clarke, G.N.; Martic, M.; Garrett, C.; Baker, H.W. Frequency of disordered zona pellucida (ZP)-induced acrosome reaction in infertile men with normal semen analysis and normal spermatozoa-ZP binding. *Hum Reprod* **2001,** *16*, 1185-90, https://doi.org/10.1093/humrep/16.6.1185.
6. Izadi, M.; Khalili, M.A.; Salehi-Abargouei, A.; Rezvani, M.E.; Aflatoonian, B. Use of zona pellucida-bound spermatozoa as a natural selection in improvement of ICSI outcomes: A systematic review and meta-analysis. *Andrologia* **2021,** *53*, https://doi.org/10.1111/and.14022.
7. Ashrafzadeh, A.; Karsani, S.A.; Nathan, S. Mammalian sperm fertility related proteins. *Int J Med Sci* **2013,** *10*, 1649-57, https://doi.org/10.7150/ijms.6395.
8. Liu, D.Y.; Zhong, Y.; Wen, Z.-N. Zona Binding: Competitive Sperm-Binding Assay. In: *Manual of Sperm Function Testing in Human Assisted Reproduction*. Majzoub, A.; Agarwal, A.; Henkel, R. Eds.; Cambridge University Press: Cambridge, **2021**; pp. 93-99, https://doi.org/10.1017/9781108878715.014.
9. Kumar, N.; Singh, N.K. An Insight into Novel Sperm Cell Proteins as Bio-markers for Male Infertility: A Review. *Current molecular medicine* **2021**, *21*, 850-859, https://doi.org/10.2174/1566524021666210121142612.
10. Gupta, S.K. Human Zona Pellucida Glycoproteins: Binding Characteristics With Human Spermatozoa and Induction of Acrosome Reaction. *Front Cell Dev Biol* **2021,** *9*, https://doi.org/10.3389/fcell.2021.619868.
11. Tumova, L.; Zigo, M.; Sutovsky, P.; Sedmikova, M.; Postlerova, P. Ligands and Receptors Involved in the Sperm-Zona Pellucida Interactions in Mammals. *Cells* **2021,** *10*, https://doi.org/10.3390/cells10010133.
12. Hamze Araujo, J.G. Development, validation and in vitro applications of novel 3D models to study gamete interaction in mammals. *Proyecto de investigación:* **2020**.
13. Rubel, M.S.; Fedotov, S.A.; Grizel, A.V.; Sopova, J.V.; Malikova, O.A.; Chernoff, Y.O.; Rubel, A.A. Functional Mammalian Amyloids and Amyloid-Like Proteins. *Life (Basel)* **2020,** *10*, https://doi.org/10.3390/life10090156.
14. Fahrenkamp, E.; Algarra, B.; Jovine, L. Mammalian egg coat modifications and the block to polyspermy. *Mol Reprod Dev* **2020,** *87*, 326-340, https://doi.org/10.1002/mrd.23320.
15. Evans, J.P. Preventing polyspermy in mammalian eggs—Contributions of the membrane block and other mechanisms. *Molecular reproduction and development* **2020,** *87*, 341-349, https://doi.org/10.1002/mrd.23331.
16. Yoshida, M.; Kawano, N.; Yoshida, K. Control of sperm motility and fertility: diverse factors and common mechanisms. *Cell Mol Life Sci* **2008,** *65*, 3446-57, https://doi.org/10.1007/s00018-008-8230-z.
17. Young, C.; Grasa, P.; Coward, K.; Davis, L. C.; Parrington, J. Phospholipase C zeta undergoes dynamic changes in its pattern of localization in sperm during capacitation and the acrosome reaction. *Fertil Steril* **2009,** *91*, 2230-42, https://doi.org/10.1016/j.fertnstert.2008.05.021.
18. Soriano-Úbeda, C.; García-Vázquez, F. A.; Matás, C. *Biotechnologies Applied to Animal Reproduction*. Apple Academic Press, **2020**.
19. Gacem, S. Universitat Autònoma de Barcelona, **2021.**
20. Aitken, R.J.; Nixon, B.; Lin, M.; Koppers, A.J.; Lee, Y.H.; Baker, M.A. Proteomic changes in mammalian spermatozoa during epididymal maturation. *Asian. J. Androl.* **2007,** *9*, 554-64, https://doi.org/10.1111/j.1745-7262.2007.00280.x.
21. Nixon, B.; Anderson, A.L.; Bromfield, E.G.; Martin, J.H.; Cafe, S.L.; Skerrett-Byrne, D.A.; Dun, M.D.; Eamens, A.L.; De Iuliis, G.N.; Johnston, S.D. Post-testicular sperm maturation in the saltwater crocodile Crocodylus porosus: assessing the temporal acquisition of sperm motility. *Reprod Fertil Dev* **2021**, *33*, 530-539, https://doi.org/10.1071/RD20204.
22. Hamze, J.G.; Sanchez, J.M.; O'Callaghan, E.; McDonald, M.; Bermejo-Alvarez, P.; Romar, R.; Lonergan, P.; Jimenez-Movilla, M. JUNO protein coated beads: A potential tool to predict bovine sperm fertilizing ability. *Theriogenology* **2020,** *155*, 168-175, https://doi.org/10.1016/j.theriogenology.2020.05.025.
23. Barbaux, S.; Ialy-Radio, C.; Chalbi, M.; Dybal, E.; Homps-Legrand, M.; Do Cruzeiro, M.; Vaiman, D.; Wolf, J.-P.; Ziyyat, A. Sperm SPACA6 protein is required for mammalian Sperm-Egg Adhesion/Fusion. *Scientific reports* **2020,** *10*, 1-15, https://doi.org/10.1038/s41598-020-62091-y.
24. de Las Mercedes Carro, M.; Peñalva, D.A.; Antollini, S.S.; Hozbor, F.A.; Buschiazzo, J. Cholesterol and desmosterol incorporation into ram sperm membrane before cryopreservation: Effects on membrane biophysical properties and sperm quality. *Biochimica et Biophysica Acta (BBA)-Biomembranes* **2020,** *1862*, https://doi.org/10.1016/j.bbamem.2020.183357.
25. Deneke, V.E.; Pauli, A. The Fertilization Enigma: How Sperm and Egg Fuse. *Annual Review of Cell and Developmental Biology* **2021,** *37*, 391-414, https://doi.org/10.1146/annurev-cellbio-120219-021751.
26. Siu, K.K.; Serrao, V.H.B.; Ziyyat, A.; Lee, J.E. The cell biology of fertilization: Gamete attachment and fusion. *J Cell Biol* **2021,** *220*, https://doi.org/10.1083/jcb.202102146.
27. Zhang, J.; Wu, J.; Huo, R.; Mao, Y.; Lu, Y.; Guo, X.; Liu, J.; Zhou, Z.; Huang, X.; Sha, J. ERp57 is a potential biomarker for human fertilization capability. *Mol Hum Reprod* **2007,** *13*, 633-9, https://doi.org/10.1093/molehr/gam049.

28. Camargo, L.S.D. Imunolocalização da osteopontina e assinaturas proteômicas do trato reprodutor de cães. *Repositorio Institucional UNESP* **2020**.
29. Tamessar, C.T.; Trigg, N.A.; Nixon, B.; Skerrett-Byrne, D.A.; Sharkey, D.J.; Robertson, S.A.; Bromfield, E.G.; Schjenken, J.E. Roles of male reproductive tract extracellular vesicles in reproduction. *Am J Reprod Immunol* **2021,** *85*, https://doi.org/10.1111/aji.13338.
30. Frickel, E.M.; Frei, P.; Bouvier, M.; Stafford, W. F.; Helenius, A.; Glockshuber, R.; Ellgaard, L. ERp57 is a multifunctional thiol-disulfide oxidoreductase. *J Biol Chem* **2004,** *279*, 18277-87, https://doi.org/10.1074/jbc.M314089200.
31. Turano, C.; Gaucci, E.; Grillo, C.; Chichiarelli, S. ERp57/GRP58: a protein with multiple functions. *Cell Mol Biol Lett* **2011,** *16*, 539-63, https://doi.org/10.2478/s11658-011-0022-z.
32. Feige, M.J.; Hendershot, L.M. Disulfide bonds in ER protein folding and homeostasis. *Curr Opin Cell Biol* **2011,** *23*, 167-75, https://doi.org/10.1016/j.ceb.2010.10.012.
33. Gaucci, E.; Raimondo, D.; Grillo, C.; Cervoni, L.; Altieri, F.; Nittari, G.; Eufemi, M.; Chichiarelli, S. Analysis of the interaction of calcitriol with the disulfide isomerase ERp57. *Sci Rep* **2016,** *6*, https://doi.org/10.1038/srep37957.
34. Zmijewski, M.A.; Carlberg, C. Vitamin D receptor (s): In the nucleus but also at membranes? *Experimental Dermatology* **2020,** *29*, 876-884, https://doi.org/10.1111/exd.14147.
35. De Silva, W.G.M.; Abboud, M.; Yang, C.; Dixon, K.M.; Rybchyn, M.S.; Mason, R.S. *Sunlight, Vitamin D and Skin Cancer*. Springer, **2020**.
36. Lv, L.; Tan, X.; Peng, X.; Bai, R.; Xiao, Q.; Zou, T.; Tan, J.; Zhang, H.; Wang, C. The relationships of vitamin D, vitamin D receptor gene polymorphisms, and vitamin D supplementation with Parkinson's disease. *Translational Neurodegeneration* **2020,** *9*, 1-13, https://doi.org/10.1186/s40035-020-00213-2.
37. Ellerman, D.A.; Myles, D.G.; Primakoff, P. A role for sperm surface protein disulfide isomerase activity in gamete fusion: evidence for the participation of ERp57. *Dev Cell* **2006,** *10*, 831-7, https://doi.org/10.1016/j.devcel.2006.03.011.
38. Wadood, A.A.; Wang, J.; Pu, L.; Shahzad, Q.; Waqas, M.; Liu, X.; Xie, L.; Yu, L.; Chen, D.; Akhtar, R.W.; Lu, Y. Proteomic Analysis Identifies Potential Markers for Chicken Primary Follicle Development. *Animals* **2021**, *11*, https://doi.org/10.3390/ani11041108.
39. Luongo, C.; Gonzalez-Brusi, L.; Cots-Rodriguez, P.; Izquierdo-Rico, M.J.; Aviles, M.; Garcia-Vazquez, F.A. Sperm Proteome after Interaction with Reproductive Fluids in Porcine: From the Ejaculation to the Fertilization Site. *Int J Mol Sci* **2020,** *21*, https://doi.org/10.3390/ijms21176060.
40. Ziyyat, A.; Rubinstein, E.; Monier-Gavelle, F.; Barraud, V.; Kulski, O.; Prenant, M.; Boucheix, C.; Bomsel, M.; Wolf, J.P. CD9 controls the formation of clusters that contain tetraspanins and the integrin alpha 6 beta 1, which are involved in human and mouse gamete fusion. *J Cell Sci* **2006,** *119*, 416-24, https://doi.org/10.1242/jcs.02730.
41. Tan, M.; Damen, M.J.; Stout, T.A.; Roelen, B.A.; Wu, W. Plasma membrane (phospho) proteome dynamics during mammalian oocyte meiosis and fertilization. *Maternal control of early mammalian embryogenesis* **1988**, *83*.
42. Lin, S.; Ke, M.; Zhang, Y.; Yan, Z.; Wu, J. Structure of a mammalian sperm cation channel complex. *Nature* **2021,** *595*, 746-750, https://doi.org/10.1038/s41586-021-03742-6.
43. Aureli, C.; Gaucci, E.; Arcangeli, V.; Grillo, C.; Eufemi, M.; Chichiarelli, S. ERp57/PDIA3 binds specific DNA fragments in a melanoma cell line. *Gene* **2013,** *524*, 390-5, https://doi.org/10.1016/j.gene.2013.04.004.
44. Bikle, D.D. In: *Principles of Bone Biology*. Elsevier, **2020**.
45. Maattanen, P.; Kozlov, G.; Gehring, K.; Thomas, D.Y. ERp57 and PDI: multifunctional protein disulfide isomerases with similar domain architectures but differing substrate-partner associations. *Biochem Cell Biol* **2006,** *84*, 881-9, https://doi.org/10.1139/o06-186.
46. Corbett, S.T.; Hill, O.; Nangia, A.K. Vitamin D receptor found in human sperm. *Urology* **2006,** *68*, 1345-9, https://doi.org/10.1016/j.urology.2006.09.011.
47. Lerchbaum, E.; Obermayer-Pietsch, B. Vitamin D and fertility: a systematic review. *Eur J Endocrinol* **2012,** *166*, 765-78, https://doi.org/10.1530/EJE-11-0984.
48. Parikh, G.; Varadinova, M.; Suwandhi, P.; Araki, T.; Rosenwaks, Z.; Poretsky, L.; Seto-Young, D. Vitamin D regulates steroidogenesis and insulin-like growth factor binding protein-1 (IGFBP-1) production in human ovarian cells. *Horm Metab Res* **2010,** *42*, 754-7, https://doi.org/10.1055/s-0030-1262837.
49. Uhland, A. M.; Kwiecinski, G. G.; DeLuca, H. F. Normalization of serum calcium restores fertility in vitamin D-deficient male rats. *J Nutr* **1992,** *122*, 1338-44, https://doi.org/10.1093/jn/122.6.1338.
50. Dcunha, R.; Hussein, R.S.; Ananda, H.; Kumari, S.; Adiga, S.K.; Kannan, N.; Zhao, Y.; Kalthur, G. Current Insights and Latest Updates in Sperm Motility and Associated Applications in Assisted Reproduction. *Reprod Sci* **2022**, **29,** 7-25, https://doi.org/10.1007/s43032-020-00408-y.
51. Maghsoumi-Norouzabad, L.; Zare Javid, A.; Mansoori, A.; Dadfar, M.; Serajian, A. The effects of Vitamin D3 supplementation on Spermatogram and endocrine factors in asthenozoospermia infertile men: a randomized, triple blind, placebo-controlled clinical trial. *Reprod Biol Endocrinol* **2021,** *19*, https://doi.org/10.1186/s12958-021-00789-y.

52. Liao, R.X.; Yu, M.; Jiang, Y.; Xia, W. Management of osteoporosis with calcitriol in elderly Chinese patients: a systematic review. *Clin Interv Aging* **2014,** *9*, 515-26, https://doi.org/10.2147/CIA.S40465.
53. Moe, S.M. Disorders involving calcium, phosphorus, and magnesium. *Prim Care* **2008,** *35*, 215-37, https://doi.org/10.1016/j.pop.2008.01.007.
54. Cheskis, B.J.; Freedman, L.P.; Nagpal, S. Vitamin D receptor ligands for osteoporosis. *Curr Opin Investig Drugs* **2006,** *7*, 906-11.
55. Pludowski, P.; Holick, M.F.; Pilz, S.; Wagner, C.L.; Hollis, B.W.; Grant, W.B.; Shoenfeld, Y.; Lerchbaum, E.; Llewellyn, D.J.; Kienreich, K.; Soni, M. Vitamin D effects on musculoskeletal health, immunity, autoimmunity, cardiovascular disease, cancer, fertility, pregnancy, dementia and mortality-a review of recent evidence. *Autoimmun Rev* **2013,** *12*, 976-89, https://doi.org/10.1016/j.autrev.2013.02.004.
56. Bouillon, R.; Okamura, W.H.; Norman, A.W. Structure-function relationships in the vitamin D endocrine system. *Endocr Rev* **1995,** *16*, 200-57, https://doi.org/10.1210/edrv-16-2-200.
57. Maestro, M.A.; Molnar, F.; Carlberg, C. Vitamin D and Its Synthetic Analogs. *J Med Chem* **2019,** *62*, 6854-6875, https://doi.org/10.1021/acs.jmedchem.9b00208.
58. Shen, X.L.; Takimoto-Kamimura, M.; Wei, J.; Gao, Q.Z. Computer-aided de novo ligand design and docking/molecular dynamics study of vitamin D receptor agonists. *J Mol Model* **2012,** *18*, 203-12, https://doi.org/10.1007/s00894-011-1066-8.
59. Demin, S.; Van Haver, D.; Vandewalle, M.; De Clercq, P.J.; Bouillon, R.; Verstuyf, A. Synthesis and biological activity of 22-oxa CD-ring modified analogues of 1alpha,25-dihydroxyvitamin D3: cis-perhydrindane CE-ring analogues. *Bioorg Med Chem Lett* **2004,** *14*, 3885-8, https://doi.org/10.1016/j.bmcl.2004.05.067.
60. Dong, G.; Wearsch, P.A.; Peaper, D.R.; Cresswell, P.; Reinisch, K.M. Insights into MHC class I peptide loading from the structure of the tapasin-ERp57 thiol oxidoreductase heterodimer. *Immunity* **2009,** *30*, 21-32, https://doi.org/10.1016/j.immuni.2008.10.018.
61. Morris, G.M.; Huey, R.; Lindstrom, W.; Sanner, M.F.; Belew, R.K.; Goodsell, D.S.; Olson, A.J. AutoDock4 and AutoDockTools4: Automated docking with selective receptor flexibility. *J Comput Chem* **2009,** *30*, 2785-91, https://doi.org/10.1002/jcc.21256.
62. Azizian, H.; Nabati, F.; Sharifi, A.; Siavoshi, F.; Mahdavi, M.; Amanlou, M. Large-scale virtual screening for the identification of new Helicobacter pylori urease inhibitor scaffolds. *J Mol Model* **2012,** *18*, 2917-27, https://doi.org/10.1007/s00894-011-1310-2.
63. Trott, O.; Olson, A.J. AutoDock Vina: improving the speed and accuracy of docking with a new scoring function, efficient optimization, and multithreading. *J Comput Chem* **2010,** *31*, 455-61, https://doi.org/10.1002/jcc.21334.
64. Wolber, G.; Langer, T. LigandScout: 3-D pharmacophores derived from protein-bound ligands and their use as virtual screening filters. *J Chem Inf Model* **2005,** *45*, 160-9, https://doi.org/10.1021/ci049885e.
65. Pronk, S.; Páll, S.; Schulz, R.; Larsson, P.; Bjelkmar, P.; Apostolov, R.; Shirts, M.R.; Smith, J.C.; Kasson, P.M.; van der Spoel, D.; Hess, B.; Lindahl, E. GROMACS 4.5: a high-throughput and highly parallel open source molecular simulation toolkit. *Bioinformatics* **2013,** *29*, 845-54, https://doi.org/10.1093/bioinformatics/btt055.
66. Schuttelkopf, A.W.; van Aalten, D.M. PRODRG: a tool for high-throughput crystallography of protein-ligand complexes. *Acta Crystallogr D Biol Crystallogr* **2004,** *60*, 1355-63, https://doi.org/10.1107/S0907444904011679.
67. Iorga, B.; Herlem, D.; Barre, E.; Guillou, C. Acetylcholine nicotinic receptors: finding the putative binding site of allosteric modulators using the "blind docking" approach. *J Mol Model* **2006,** *12*, 366-72, https://doi.org/10.1007/s00894-005-0057-z.
68. Hetenyi, C.; van der Spoel, D. Blind docking of drug-sized compounds to proteins with up to a thousand residues. *FEBS Lett* **2006,** *580*, 1447-50, https://doi.org/10.1016/j.febslet.2006.01.074.
69. Tohda, C.; Urano, T.; Umezaki, M.; Nemere, I.; Kuboyama, T. Diosgenin is an exogenous activator of 1,25D(3)-MARRS/Pdia3/ERp57 and improves Alzheimer's disease pathologies in 5XFAD mice. *Sci Rep* **2012,** *2*, https://doi.org/10.1038/srep00535.
70. Gezen-Ak, D.; Yilmazer, S.; Dursun, E. Why vitamin D in Alzheimer's disease? The hypothesis. *J Alzheimers Dis* **2014,** *40*, 257-69, https://doi.org/10.3233/JAD-131970.
71. Doryanizadeh, L.; Morshed-Behbahani, B.; Parsanezhad, M.E.; Dabbaghmanesh, M.H.; Jokar, A. Calcitriol Effect on Outcomes of in Vitro Fertilization in Infertile Women with Vitamin D Deficiency: A Double-Blind Randomized Clinical Trial. *Z Geburtshilfe Neonatol* **2021,** *225*, 226-231, https://doi.org/10.1055/a-1206-1064.
72. Tiwari, A. Elocalcitol, a vitamin D3 analog for the potential treatment of benign prostatic hyperplasia, overactive bladder and male infertility. *IDrugs* **2009,** *12*, 381-93.